THE UNIVERSITY OF RHODE ISLAND

University of Rhode Island
DigitalCommons@URI

Graduate School of Oceanography Faculty Publications

Graduate School of Oceanography

4-1-2023

Patterns in sources and forms of nitrogen in a large eutrophic lake during a cyanobacterial harmful algal bloom

Jenan J. Kharbush
University of Michigan, Ann Arbor

Rebecca S. Robinson
University of Rhode Island

Susan J. Carter
Harvard University

Follow this and additional works at: https://digitalcommons.uri.edu/gsofacpubs

Citation/Publisher Attribution

Kharbush, Jenan J., Rebecca S. Robinson, and Susan J. Carter. "Patterns in sources and forms of nitrogen in a large eutrophic lake during a cyanobacterial harmful algal bloom." *Limnology and Oceanography* 68, 4 (2023). doi: 10.1002/lno.12311.

This Article is brought to you by the University of Rhode Island. It has been accepted for inclusion in Graduate School of Oceanography Faculty Publications by an authorized administrator of DigitalCommons@URI. For more information, please contact digitalcommons-group@uri.edu. For permission to reuse copyrighted content, contact the author directly.

Patterns in sources and forms of nitrogen in a large eutrophic lake during a cyanobacterial harmful algal bloom

Creative Commons License

This work is licensed under a Creative Commons Attribution 4.0 License.

This article is available at DigitalCommons@URI: https://digitalcommons.uri.edu/gsofacpubs/2192

Check for updates

LIMNOLOGY and OCEANOGRAPHY

ASLO

Limnol. Oceanogr. 68, 2023, 803–815
© 2023 The Authors. *Limnology and Oceanography* published by Wiley Periodicals LLC on behalf of Association for the Sciences of Limnology and Oceanography.
doi: 10.1002/lno.12311

Patterns in sources and forms of nitrogen in a large eutrophic lake during a cyanobacterial harmful algal bloom

Jenan J. Kharbush,[1*] **Rebecca S. Robinson**,[2] **Susan J. Carter**[3]

[1]Department of Earth and Environmental Sciences, University of Michigan, Ann Arbor, Michigan
[2]Graduate School of Oceanography, University of Rhode Island, Narragansett, Rhode Island
[3]Department of Earth and Planetary Sciences, Harvard University, Cambridge, Massachusetts

Abstract

Western Lake Erie experiences an annual, toxic cyanobacterial harmful algal bloom (cyanoHAB), primarily caused by excess anthropogenic inputs of nitrogen (N) and phosphorous (P). Because the non-N fixing cyanobacteria species *Microcystis* dominates these blooms, N availability is hypothesized to play a central role in cyanoHAB progression, as well as production of the N-rich toxin microcystin. Many previous studies focused on nitrate because it is the most abundant N substrate during bloom initiation. However, recent work implicated reduced N substrates like ammonium and dissolved organic N (DON) in promoting greater bloom biomass and longevity. To examine the relative importance of oxidized and reduced N substrates to phytoplankton during different bloom stages, we measured concentrations and natural abundance $\delta^{15}N$ isotope values of dissolved N substrates and phytoplankton biomass throughout the entirety of the 2020 cyanoHAB in Western Lake Erie. The results provide the first data on DON dynamics and composition in Western Lake Erie, and suggest that phytoplankton, including *Microcystis*, likely relied on N regenerated from the DON pool in later bloom stages. In addition, the stable isotope data confirm the importance of nitrate delivered via the Maumee River to cyanobacterial growth and toxin production.

The increasing occurrence of toxin-producing cyanobacterial harmful algal blooms (cyanoHABs) in freshwaters (Hou et al. 2022) is a major concern for drinking water quality and security. Blooms now occur annually in most of the Laurentian Great Lakes, which supply 84% of surface freshwater in North America. In Lake Erie, the shallowest and most productive of the Great Lakes, an annual summer cyanoHAB has occurred in the western basin for the last three decades. Nitrogen (N) and phosphorous (P) delivered to the lake via the Detroit, Maumee, and Sandusky rivers (Allinger and Reavie 2013) are mostly derived from nonpoint agricultural runoff (Maccoux et al. 2016; Scavia et al. 2016), and promote blooms of toxigenic cyanobacteria like *Microcystis aeruginosa*, which produce the hepatotoxic cyclic peptides known as microcystins.

In Lake Erie and other lakes affected by cyanoHABs, annual P loading is well-established as a key predictor of overall bloom size (Kane et al. 2014; Stumpf et al. 2016), and therefore most management strategies focus on P (GLWQA 2016). However, N availability is an important driving factor for cyanoHABs dominated by nondiazotrophic cyanobacteria such as *Microcystis*, which rely on fixed N substrates present in chemically oxidized (nitrate, NO_3^- and nitrite, NO_2^-), and reduced forms (ammonium, NH_4^+, and dissolved organic nitrogen DON, including urea). Most phytoplankton use NH_4^+ before other N substrates, because NH_4^+ requires less energy to assimilate into cellular biomass (Flores and Herrero 2005). However, in most freshwater systems NO_3^- is more abundant than NH_4^+ (Durand et al. 2011), and *Microcystis* can use multiple forms of N, even in the presence of NH_4^+ (Chaffin and Bridgeman 2014; Belisle et al. 2016). Although total N loads have not increased since the 1990s (Kane et al. 2014; Stow et al. 2015), and there is no correlation between NO_3^- concentrations and bloom biomass (Kane et al. 2014), the proportion of non-nitrate or reduced N has increased in recent decades and is significantly, positively correlated with bloom biomass (Newell et al. 2019). Nondiazotrophic cyanobacteria have a strong affinity for reduced N substrates, allowing them to outcompete eukaryotic

*Correspondence: jenanjk@umich.edu

This is an open access article under the terms of the Creative Commons Attribution License, which permits use, distribution and reproduction in any medium, provided the original work is properly cited.

Additional Supporting Information may be found in the online version of this article.

Author Contribution Statement: J.J.K. conceptualized the study, collected the water samples, and analyzed data. R.S.R. measured and processed the dissolved nitrogen isotope data. S.J.C. collected and processed bulk isotope data. J.J.K. wrote the initial manuscript, which was then revised with feedback from all authors.

taxa, especially for NH_4^+ (Blomqvist et al. 1994; Glibert et al. 2016). This suggests an important role for external loading of reduced N, as well as internal lake recycling, in promoting and sustaining cyanoHABs.

N availability and speciation is also important because cellular N status (i.e., N-replete vs. N-limited) influences microcystin toxin production. In culture studies with *Microcystis*, greater N availability resulted in increased expression of microcystin biosynthetic genes (Harke and Gobler 2015) or increased cellular microcystin quotas (Downing et al. 2005; Horst et al. 2014). Compared with P additions, N additions to natural communities resulted in a greater increase in microcystin concentrations (Davis et al. 2015; Jankowiak et al. 2019), and the greatest concentrations occurred under conditions of excess N relative to P (Beversdorf et al. 2015). Furthermore, because not all strains of *Microcystis* produce microcystins, toxin concentrations can depend on which strains are present. In Lake Erie and other cyanoHAB-affected lakes, toxin concentrations are often higher in early or peak stages of the bloom and decrease during later bloom stages, despite persistence of dense cyanobacterial biomass (Gobler et al. 2016; Berry et al. 2017). This is attributed to a community shift from dominantly toxigenic to nontoxigenic strains (Davis et al. 2009; Yancey et al. 2022), but the environmental drivers of this transition are unresolved. In Lake Erie, the relative abundance of toxic genotypes is positively correlated with NO_3^- concentrations (Yancey et al. 2022), and the greatest toxin concentrations seem to occur just after the seasonal peak in NO_3^- concentrations (Gobler et al. 2016; Berry et al. 2017). Therefore, N availability may directly influence the population dynamics of toxigenic and nontoxigenic strains. NO_3^- is drawn down to low concentrations by late summer (Chaffin et al. 2013), and toxin concentration tends to decline after that point. However, cyanobacterial biomass often remains high well into the fall. *Microcystis* must therefore be relying on other N sources after NO_3^- is consumed, such as labile components of DON or regenerated NH_4^+ (Hampel et al. 2019).

The form of bioavailable N can also affect bloom toxin concentrations by influencing production of different microcystin structures (congeners), which vary in toxicity (Chernoff et al. 2020). In contrast to the results above that link NO_3^- with increased toxin concentrations, other studies observed that adding reduced N compounds like NH_4^+ or urea to natural communities increased microcystin production (Donald et al. 2011; Davis et al. 2015). In a study that examined three eutrophic lakes prone to blooms, total N, NH_4^+, and DON concentrations all influenced the cyanobacterial community and congener composition, and DON in particular was positively correlated with *Microcystis* biomass (Monchamp et al. 2014). In many freshwater systems DON is a large proportion of the total dissolved N pool (Berman and Bronk 2003; Yao et al. 2020), but very little is known about DON in Lake Erie, including how its concentration compares to other frequently measured N sources like NO_3^- and NH_4^+, and whether this evolves during the bloom.

Evidence thus far points to a central role of N in cyanoHAB dynamics. An open question is whether the type of N substrate available influences bloom progression. In particular, the importance of DON to cyanobacterial growth and toxin production is unknown. The stable isotope "fingerprints" of N substrates and particulate organic matter (POM) can provide insight into this question, by tracing the sources and incorporation of N by phytoplankton during the bloom. This is possible because each pool of N (e.g., NO_3^-, NH_4^+, POM) often has a distinct range of $\delta^{15}N$ values (Lehmann et al. 2004; Kendall et al. 2007), which are determined by the $\delta^{15}N$ composition of the N source and any subsequent isotopically fractionating reactions. These include biological transformations that convert one N form into another, such as nitrification, uptake or assimilation, and remineralization, which impart characteristic changes in $\delta^{15}N$ values (Sigman et al. 2009). Examining the magnitude and direction of changes in $\delta^{15}N$ values between pools of N, such as between N substrates and POM, can inform on N cycling processes occurring between stations or over time.

This paper reports concentrations and N isotope composition of N substrates in Western Lake Erie during the 2020 cyanoHAB, including the first measurements of DON concentrations and isotope composition. The N isotope compositions of POM and dissolved N substrates provide insight into which N sources contribute to bloom biomass and potentially to toxin production.

Methods

Sample collection

Samples were collected approximately weekly between mid-June and late September 2020, from three stations in the western basin of Lake Erie (Fig. 1). The stations form a transect extending offshore and correspond to NOAA-Great Lakes Environmental Research Laboratory (NOAA-GLERL) long-term monitoring Stas. WE9 (Maumee Bay), WE2 (Nearshore), and WE4 (Offshore). The water column depths differ between stations: 2.7, 5.7, and 8.9 m, for WE9, WE2, and WE4, respectively. Because of pandemic-related restrictions, WE4 could not be sampled until July. Water samples were collected from 0 to 1 m below the surface using a peristaltic pump and tubing, then transported in carboys back to the lab. In the lab, POM was collected by vacuum filtering 2 liters of water through precombusted glass fiber filters (GFFs, Cytiva-Whatman, 0.7 μm nominal pore size). Filters were frozen at −80°C, and the filtrate was subsequently filtered through 0.2-μm polyethersulfone flat filters (Millipore Express PLUS) and collected for nutrient and fluorescence analysis. Nutrient samples were frozen at −20°C until analysis, while fluorescence samples were stored at 4°C. All water samples were filtered and stored on the same day they were collected.

19395590, 2023, 4, Downloaded from https://aslopubs.onlinelibrary.wiley.com/doi/10.1002/lno.12311 by Wheaton College Ma, Wiley Online Library on [07/11/2024]. See the Terms and Conditions (https://onlinelibrary.wiley.com/terms-and-conditions) on Wiley Online Library for rules of use; OA articles are governed by the applicable Creative Commons License

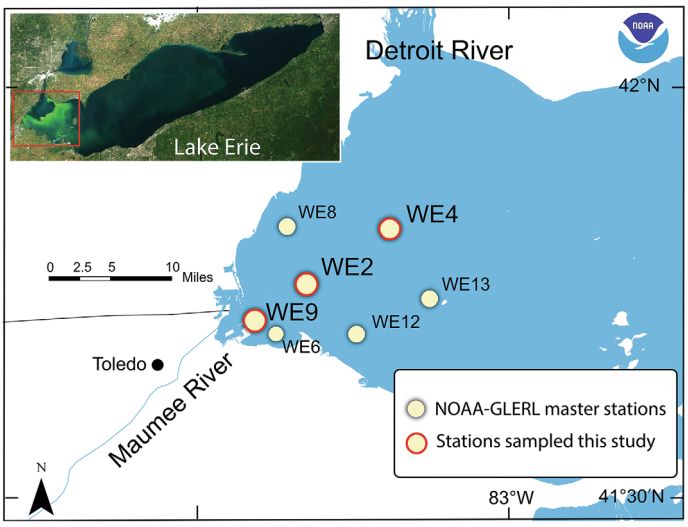

Fig. 1. NOAA-GLERL master stations in Lake Erie and selected stations monitored during this study. Water column depths are 2.7, 5.7, and 8.9 m for WE9, WE2, and WE4, respectively.

Phytoplankton community composition

Phytoplankton community composition was estimated using a submersible Fluoroprobe (bbe Moldaenke GmbH, Germany) which monitors in situ chlorophyll fluorescence. The Fluoroprobe quantifies four broad groups of chlorophyll *a*-containing phytoplankton (Beutler et al. 2002; Escoffier et al. 2015): (1) green algae, (2) cyanobacteria, (3) diatoms, and (4) cryptophytes. Fluorescence profiles for each group were depth-integrated and normalized to total chlorophyll concentrations to give the fraction of chlorophyll contributed by each group. Uncertainty in classification of each phytoplankton group by Fluoroprobe is estimated as ± 5% (Escoffier et al. 2015).

Nutrient concentration and $\delta^{15}N$ analysis

Dissolved nutrient and microcystin concentrations were determined at the Cooperative Institute for Great Lakes Research at University of Michigan. The 2020 dataset was downloaded from NOAA National Centers for Environmental Information (Burtner et al. 2022). All N substrate concentrations are reported as μM N. Isotope values are reported as δ values, in units of permil (‰):

$$\delta\,(‰) = \left[\frac{R_{\text{sample}}}{R_{\text{standard}}}\right] \times 1000,$$

where R represents the ratio of heavy to light isotope (e.g., $^{15}N/^{14}N$) in either the sample or the standard. Data are reported relative to the international standards of air for $\delta^{15}N$, and Vienna Standard Mean Ocean Water for $\delta^{18}O$.

$\delta^{15}N$ values of NO_3^- and total dissolved N (TDN, includes NO_3^-, NO_2^-, NH_4^+, and DON) were measured using the denitrifier method (Casciotti et al., 2002; Sigman et al. 2009), on a Delta V Advantage isotope ratio mass spectrometer with a custom-built purge and trap system. Isotope measurements were standardized to the N_2 reference scale using standard reference materials IAEA N3 and USGS 34. The denitrifier method cannot distinguish between NO_3^- and NO_2^-, but NO_2^- is typically present at very low concentration in oxygenated surface waters and is therefore disregarded. TDN was measured using persulfate oxidation to NO_3^-, followed by the denitrifier method (Knapp et al. 2005, *see* Supporting Information Data S1).

Before ^{15}N analysis, the concentration of NO_3^- in both unoxidized and oxidized samples was measured using a chemiluminescent NO_x analyzer (Teledyne NO/NO_x Analyzer 200E). The concentration of DON was calculated by subtracting concentrations of NH_4^+ and NO_3^- in unoxidized samples from the NO_3^- concentration of persulfate-oxidized TDN samples. TDN concentration was corrected for any N contamination in reagents, but this was always <0.5 μM or below detection. The concentrations and $\delta^{15}N$ values of TDN and NO_3^- were used to calculate the $\delta^{15}N$ value of total reduced N ($\delta^{15}N_{TRN}$) by mass balance:

$$\delta^{15}N_{TRN} = \left(\delta^{15}N_{TDN} \times [TDN] - \delta^{15}N_{NO3} \times \left[NO_3^-\right]\right)/[TRN].$$

TRN is mostly DON, but includes some NH_4^+ as well (Supporting Information Table S1), especially at the beginning of the sampling season. We were unable to measure $\delta^{15}N$ of NH_4^+ in this study and therefore report isotope values as "$\delta^{15}N_{TRN}$" rather than "$\delta^{15}N_{DON}$" (*see* Supporting Information Data S1 for constraints on how unknown NH_4^+ $\delta^{15}N$ values may influence the calculated $\delta^{15}N$ values). The average precision for both $\delta^{15}N_{NO3}$ and $\delta^{15}N_{TDN}$ was 0.3‰, and propagation of error results in an average precision for $\delta^{15}N_{TRN}$ of 0.7‰.

$\delta^{15}N$ analysis of POM

GFFs were dried at 50°C overnight, then subsampled for ^{15}N analysis using a cork borer. Subsamples were placed into tin capsules (Costech), which were folded and crushed to remove air, and analyzed on a Thermo Scientific Flash IRMS Elemental Analyzer with EA Isolink, coupled to a Delta V Advantage IRMS through a Conflo IV interface. Sample $\delta^{15}N$ values were calculated using in-house laboratory standards as well as standard reference materials USGS40 and USGS41a.

Excitation–emission matrices fluorescence analysis

For insight into DON composition and sources, we examined fluorescence spectra of dissolved organic matter (FDOM), measured from excitation-emission matrices of 0.2 μm filtered water samples (Cory et al. 2016). We compared DON concentration and isotope values with "Peak T", the fraction of FDOM associated with amino acid or protein-like material, and "Peak A", the fraction associated with terrestrial or soil-derived organic material (Cory et al. 2016). The ratio of Peak

19395590, 2023, 4, Downloaded from https://aslopubs.onlinelibrary.wiley.com/doi/10.1002/lno.12311 by Wheaton College Ma, Wiley Online Library on [07/11/2024]. See the Terms and Conditions (https://onlinelibrary.wiley.com/terms-and-conditions) on Wiley Online Library for rules of use; OA articles are governed by the applicable Creative Commons License

T/A represents the fraction of amino acid-like relative to terrestrial material in FDOM, and higher ratios have been shown to correlate with higher bioavailability of DOM (Fellman et al. 2009).

Statistics and data

Correlation coefficients were calculated in R (v4.2.0; R Core Team 2022) using RStudio (RStudio Team 2022). The R packages dplyr (Wickham et al. 2022) and ggpubr (Kassambara 2020) were used to statistically and visually check data for normality. Because most of the environmental variables examined here did not follow a normal distribution, Spearman's rank correlation coefficient (r_s) was used to examine correlations between variables.

Results

Bloom dynamics

The timing (initiation and decline), extent, and toxin concentrations of the Lake Erie cyanoHAB vary from year to year. In 2020, the bloom was relatively mild compared to previous years, with a bloom severity index (SI) of 3.0 (NOAA-NCCOS 2020). The SI is based on the amount of biomass during the peak 30 d of the bloom, and a bloom with SI above 5.0 is considered harmful (the largest bloom, in 2015, had a SI of 10.5). The 2020 bloom began in early July, reached peak biomass levels in late August, and declined in September. Particulate microcystin concentrations were low compared to previous years, peaking in late July at 4 $\mu g\ L^{-1}$ at WE9, 2 $\mu g\ L^{-1}$ at WE2, and < 1 $\mu g\ L^{-1}$ at WE4 (Supporting Information Fig. S1). For comparison, during 2014, considered one of the most toxic blooms, microcystin concentrations reached 30 $\mu g\ L^{-1}$ at WE2 and 12 $\mu g\ L^{-1}$ at WE4 in early August. Surface scum was not observed at WE2, WE4, or WE9 during the 2020 bloom.

The phytoplankton community composition varied between stations (Supporting Information Fig. S1). Cyanobacteria comprised the majority of the community at WE9 for most of the summer, except at the beginning and end of the sampling period, when there were greater contributions from green algae and diatoms, respectively. At WE2 cyanobacteria were most dominant in late July but co-existed with both diatoms and green algae later in the season. WE4 was the least productive station, with notably lower phycocyanin, chlorophyll, and toxin concentrations, and the community consisted of mostly green algae.

Dissolved N concentrations

The nearshore Stas. WE9 and WE2 followed a similar temporal pattern in nitrate concentration ($[NO_3^-]$), with high concentrations from the spring nutrient pulse drawn down by phytoplankton uptake during June and July (Fig. 2). WE9 experienced the most variability in N concentrations, perhaps due to proximity to the Maumee River. At WE9, $[NO_3^-]$ reached a minimum concentration of 0.2 μM in early August, but concentrations increased again thereafter. At WE2, $[NO_3^-]$ reached

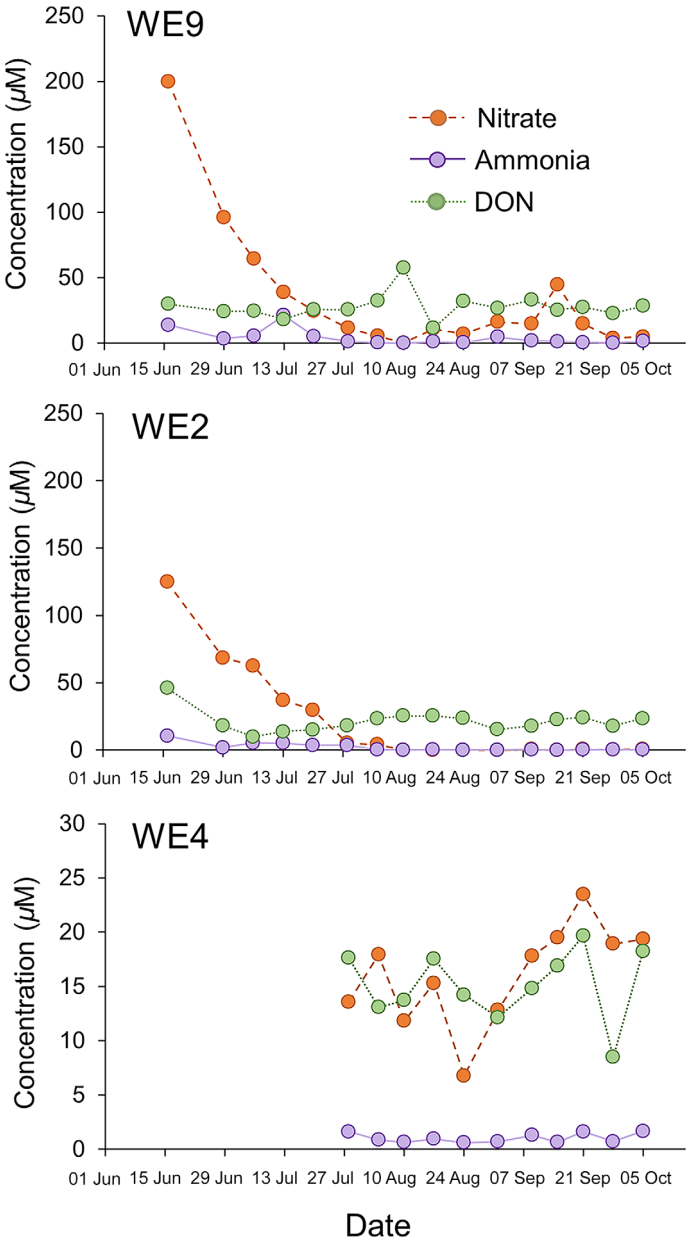

Fig. 2. Concentration of N sources by station throughout the bloom. Note the difference in scale at Sta. WE4.

a minimum of 0.07 μM in early August and remained < 1 μM for the rest of the season. Due to the delay in sampling WE4, the data does not show whether the initial peak in $[NO_3^-]$ was present, but $[NO_3^-]$ remained high relative to the other two stations with a median value of 18 μM compared to 10.8 μM at WE9 and 0.3 μM at WE2, from 7/28 forward (Fig. 2). Ammonium concentrations ($[NH_4^+]$) were very low across all three stations, with higher concentrations in early June (Fig. 2). This agrees with previous data in Lake Erie, which suggests that $[NH_4^+]$ is kept low because NH_4^+ is rapidly taken up by cyanobacteria and/or nitrifying bacteria. Because of this high bioreactivity, concentrations are not necessarily representative of

19395590, 2023, 4, Downloaded from https://aslopubs.onlinelibrary.wiley.com/doi/10.1002/lno.12311 by Wheaton College Ma, Wiley Online Library on [07/11/2024]. See the Terms and Conditions (https://onlinelibrary.wiley.com/terms-and-conditions) on Wiley Online Library for rules of use; OA articles are governed by the applicable Creative Commons License

NH_4^+ availability and utilization. Recent work measured the highest potential NH_4^+ uptake rates near the Maumee River inflow and during the peak bloom months (Hoffman et al. 2022).

DON concentration ([DON]) was calculated by subtracting $[NO_3^-/NO_2^-]$ and $[NH_4^+]$ from total dissolved N concentration, ([TDN]). In general, DON concentrations were higher at nearshore compared to offshore stations (Fig. 2; Supporting Information Table S1). At both WE9 and WE2, [DON] increases as $[NO_3^-]$ decreases, and becomes the most abundant N substrate in August and much of September, making up 50% or more of the total N pool (Fig. 2; Supporting Information Fig. S2). This pattern is most striking at WE2 where [DON] is up to 80X greater than other N substrates and close to 100% of total dissolved N. At WE4 [DON] is comparable to $[NO_3^-]$ in magnitude, with a median concentration of 14.8 μM. These temporal and spatial variations in DON concentration suggest that the DON pool is dynamic, with material added and removed throughout the season.

[DON] was positively correlated with FDOM Peak T ($r_s = 0.62$, $p = 1.75 \times 10^{-5}$; Fig. 3), which agrees with previous work showing that Peak T is composed of amino acid-like fractions of the dissolved organic matter pool, and thus is a proxy for a fraction of DON (Yamashita and Tanoue 2003). Peak T was very strongly, positively correlated with conductivity ($r_s = 0.97$, $p = 2.2 \times 10^{-16}$; Supporting Information Fig. S3), demonstrating that the Maumee River is a dominant source of this fraction of DON. The Peak T/A ratio, which represents the amount of amino acid-like relative to terrestrially derived "humic" organic material, increased with decreasing specific conductivity (Supporting Information Fig. S4), consistent with (Cory et al. 2016). According to the interpretation of Cory et al. (2016), this pattern indicates that amino acid-like material made up a greater fraction of dissolved organic matter

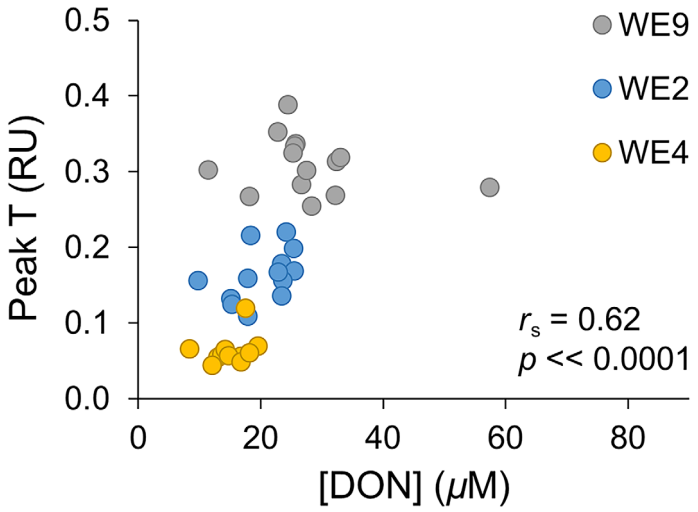

Fig. 3. Relationship between FDOM Peak T (RU = relative units) and DON concentration. The outlying gray data point corresponds to the peak in DON at Sta. WE9 on 8/10 (Fig. 2).

offshore vs. nearshore, even though total DON concentrations decreased offshore.

Patterns in $\delta^{15}N$ isotope values

There were spatial and temporal patterns in the isotope values of POM ($\delta^{15}N_{POM}$), NO_3^- ($\delta^{15}N_{NO3}$), and TRN ($\delta^{15}N_{TRN}$). $\delta^{15}N_{NO3}$ and $\delta^{15}N_{TRN}$ both had relatively higher values closer to shore and lower values offshore. $\delta^{15}N_{POM}$ values were higher at WE9, but similar between Stas. WE2 and WE4 (Table 1). Temporal patterns in $\delta^{15}N_{POM}$ were similar between WE9 and WE2, where $\delta^{15}N_{POM}$ increased throughout June and July, reached a high point in late July, and decreased in August. At WE9 $\delta^{15}N_{POM}$ increased again during September, from 5‰ in mid-August to 11‰ in mid-September (Fig. 4). In contrast, at WE2 $\delta^{15}N_{POM}$ remained between 4‰ and 5‰ from mid-August onward.

$\delta^{15}N_{TRN}$ varied throughout the bloom, suggesting that the inputs and outputs to the DON pool indicated by changing [DON] concentrations affected isotope values (Fig. 4). [DON] and $\delta^{15}N_{TRN}$ were moderately, positively correlated ($r_s = 0.63$, $p = 0.0001$). In contrast, despite rapid drawdown of NO_3^- early in the sampling period, $\delta^{15}N_{NO3}$ showed little temporal variation, and was not correlated with $[NO_3^-]$, suggesting that fractionation associated with biological uptake was not the dominant control on $\delta^{15}N_{NO3}$ values. This agrees with other studies that suggest external N sources are the major control on nitrate isotope composition in lakes (Ostrom et al. 1997; Teranes and Bernasconi 2000). The dual isotope composition of NO_3^- ($\delta^{15}N$ and $\delta^{18}O$) suggests that most nitrate in Lake Erie derives from soils, manure/sewage, and ammonia-based fertilizers, with no apparent contribution from synthetic nitrate-based fertilizers (Supporting Information Fig. S5).

$\delta^{15}N_{NO3}$ was strongly, positively correlated with specific conductivity ($r_s = 0.87$, $p = 1.5 \times 10^{-7}$), and the data form a mixing line between near and offshore stations (Fig. 5A). Specific conductivity is a proxy for riverine influence in Lake Erie (Cory et al. 2016), with higher values corresponding to Maumee River water and lower values corresponding to Detroit River water due to geological differences between the two watersheds (Sterner 2021). Higher $\delta^{15}N_{NO3}$ values are therefore associated with proximity to the Maumee River mouth. $\delta^{15}N_{POM}$ was also correlated with conductivity although the correlation was not as strong ($r_s = 0.57$, $p = 9.7 \times 10^{-5}$; Fig. 5B) and there was more overlap between stations compared with $\delta^{15}N_{NO3}$. $\delta^{15}N_{TRN}$ showed the weakest relationship with conductivity ($r_s = 0.55$, $p = 0.001$; Fig. 5C), consistent with in-lake cycling processes that changed both DON composition and isotope values.

Discussion

Phytoplankton usage of N substrates

In aquatic environments like Lake Erie where phytoplankton are the major component of POM during the summer months, $\delta^{15}N_{POM}$ is controlled by the isotope composition of

19395590, 2023, 4, Downloaded from https://aslopubs.onlinelibrary.wiley.com/doi/10.1002/lno.12311 by Wheaton College Ma, Wiley Online Library on [07/11/2024]. See the Terms and Conditions (https://onlinelibrary.wiley.com/terms-and-conditions) on Wiley Online Library for rules of use; OA articles are governed by the applicable Creative Commons License

Table 1. Median, maximum, and minimum $\delta^{15}N$ values (‰) at each station.

Station	Median $\delta^{15}N_{POM}$	Max	Min	Median $\delta^{15}N_{NO3}$	Max	Min	Median $\delta^{15}N_{TRN}$	Max	Min
WE9	8.6	12.5	5.1	8.5	11.2	7.8	4.8	7.7	2.3
WE2	5.4	9.0	4.3	7.4	7.8	5.8	4.5	5.4	−2.4
WE4	5.6	8.6	4.5	3.6	7.0	2.5	2.8	4.8	0.8

the N substrate(s) and isotope fractionation during phytoplankton uptake. $\delta^{15}N_{POM}$ therefore records an integrated signal of the N sources used by phytoplankton. We compared

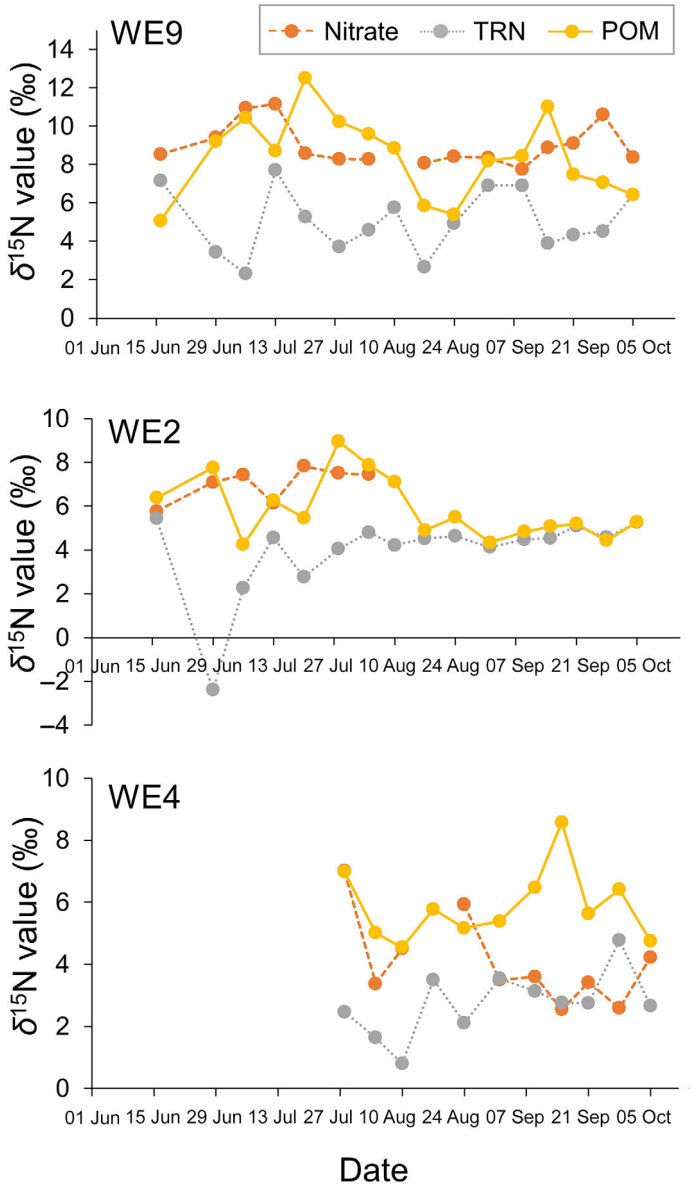

Fig. 4. $\delta^{15}N$ of nitrate (orange), TRN (gray), and POM (yellow) throughout the bloom at each station. "$\delta^{15}N_{TRN}$" may include DON and ammonium because we were unable to measure $\delta^{15}N$ of ammonium in these samples (*see* "Methods" section and Supporting Information Data S1).

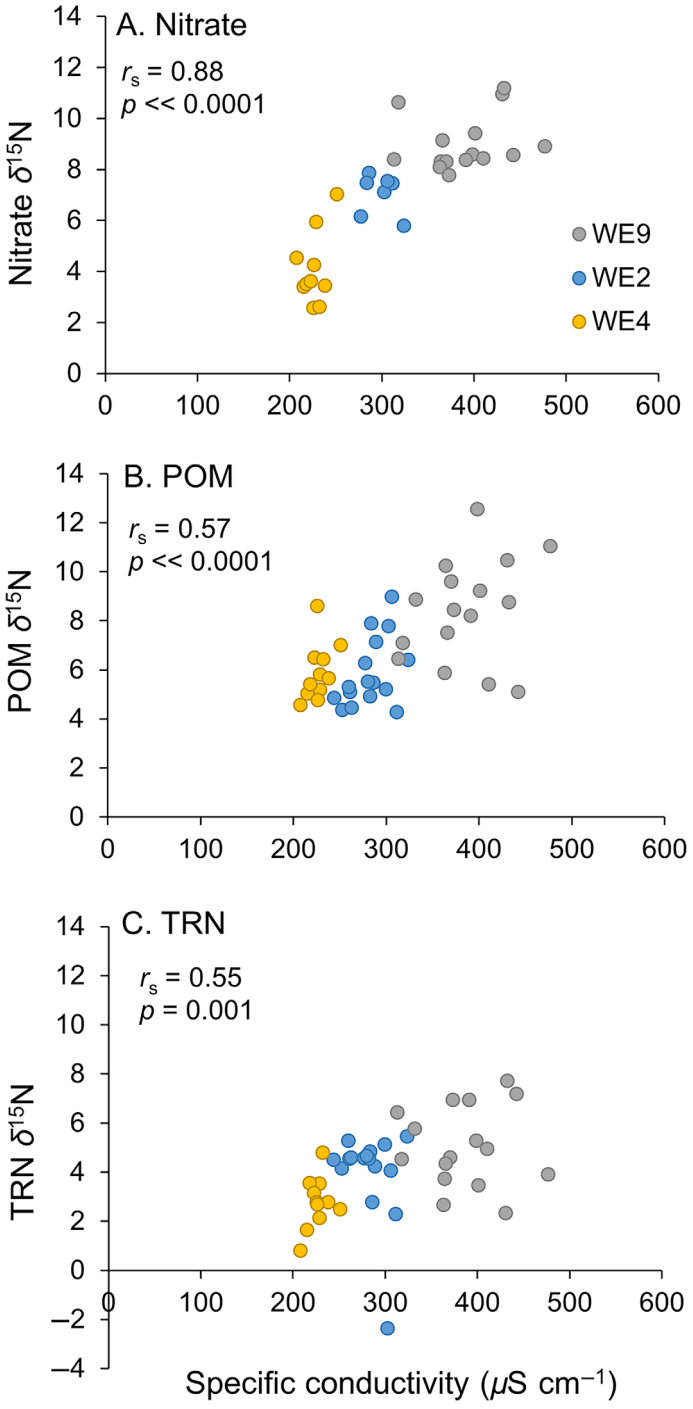

Fig. 5. Relationship between specific conductivity and $\delta^{15}N$ of (**A**) nitrate, (**B**) POM, and (**C**) TRN.

19395590, 2023, 4, Downloaded from https://aslopubs.onlinelibrary.wiley.com/doi/10.1002/lno.12311 by Wheaton College Ma, Wiley Online Library on [07/11/2024]. See the Terms and Conditions (https://onlinelibrary.wiley.com/terms-and-conditions) on Wiley Online Library for rules of use; OA articles are governed by the applicable Creative Commons License

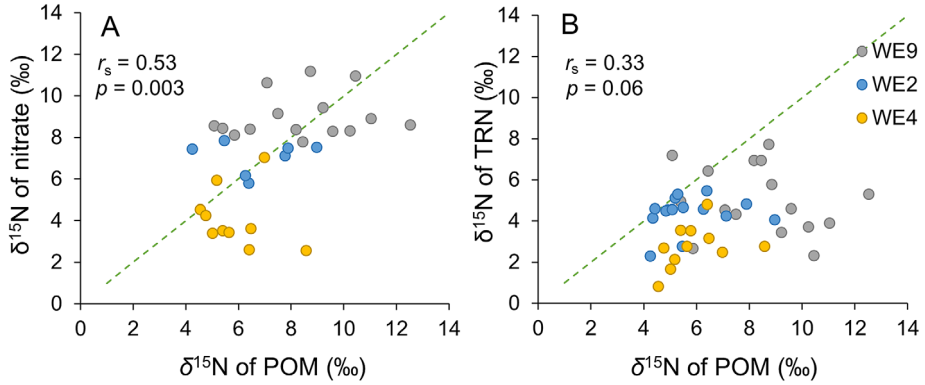

Fig. 6. Relationship between $\delta^{15}N$ of POM and (**A**) nitrate and (**B**) DON, plotted by station. Green dashed line in (**A**) and (**B**) is 1 : 1 line.

$\delta^{15}N_{POM}$ with $\delta^{15}N_{NO3}$ and $\delta^{15}N_{TRN}$ to examine whether phytoplankton used one or both of these N substrates throughout the bloom.

The isotope data suggest that NO_3^- was a more important source of N for phytoplankton than DON in two different ways. First, $\delta^{15}N_{POM}$ exhibited a stronger relationship with $\delta^{15}N_{NO3}$ ($r_s = 0.52$, $p = 0.003$) than with $\delta^{15}N_{TRN}$ ($r_s = 0.33$, $p = 0.06$; Fig. 6). Second, phytoplankton preferentially take up ^{14}N-containing material, leaving the remaining pool of N substrate enriched in ^{15}N (Fogel and Cifuentes 1993; Granger et al. 2010). Therefore, when N is not limiting, $\delta^{15}N_{POM}$ should always be lower than the $\delta^{15}N$ of the primary N substrate (Ostrom et al. 1997; McCusker et al. 1999; Finlay and Kendall 2007). For about 60% of the samples, $\delta^{15}N_{POM}$ was lower than or similar to the corresponding $\delta^{15}N_{NO3}$, but $\delta^{15}N_{TRN}$ was almost always less than or equal to $\delta^{15}N_{POM}$ (Fig. 6), supporting NO_3^- as a more important N substrate than DON for much of the bloom. Among the remaining 40% of samples that had $\delta^{15}N_{POM}$ greater than both $\delta^{15}N_{NO3}$ and $\delta^{15}N_{TRN}$, most are from Stas. WE9 and WE4. At WE9, this occurred mostly in June and July, and may reflect phytoplankton usage of isotopically heavy NH_4^+ from the Maumee River. We did not measure $\delta^{15}N$ of NH_4^+ during this study, but previously measured NH_4^+ $\delta^{15}N$ values had a median value of 12‰ (Supporting Information Table S3), which would be consistent with the high $\delta^{15}N_{POM}$ values observed here. In contrast, at

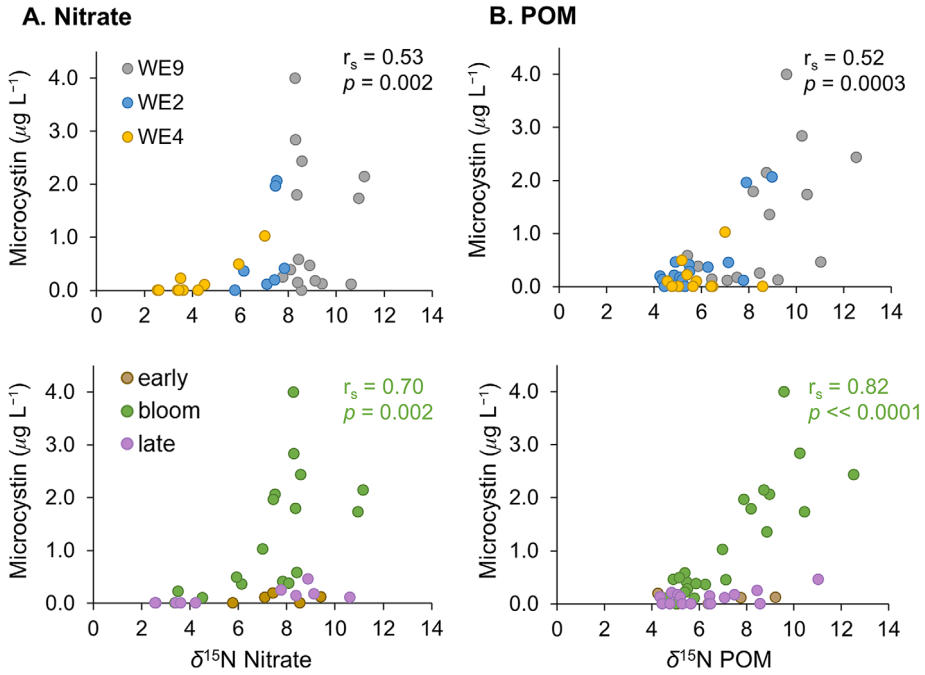

Fig. 7. Relationship between microcystin concentration and (**A**) nitrate and (**B**) POM, colored by station (top) and bloom stage (bottom). Bloom stage was based on microcystin concentration ("bloom" = when microcystin was consistently above zero, *see* Supporting Information Fig. S1). Spearman's rank correlation coefficients (r_s) are shown for all stations (black, top) and for only bloom data points (green, bottom).

19395590, 2023, 4, Downloaded from https://aslopubs.onlinelibrary.wiley.com/doi/10.1002/lno.12311 by Wheaton College Ma, Wiley Online Library on [07/11/2024]. See the Terms and Conditions (https://onlinelibrary.wiley.com/terms-and-conditions) on Wiley Online Library for rules of use; OA articles are governed by the applicable Creative Commons License

WE4 $\delta^{15}N_{POM}$ was higher relative to both NO_3^- and DON later in the summer (after 8/24, Fig. 4), and delivery of isotopically heavy ammonium seems less likely than at Sta. WE9. One possible explanation for the pattern at WE4 is advection or transport of material from elsewhere. Advection of material from WE2 is unlikely, as POM values remained low through the second part of the summer, but another possible source is material transported from the Detroit River, as WE4 is influenced by both Maumee and Detroit River water.

Despite the clear importance of nitrate during the bloom, DON became a more important N substrate for phytoplankton in later bloom stages. For example, nearly all NO_3^- was consumed at Sta. WE2 after 8/10, and $\delta^{15}N_{POM}$ and $\delta^{15}N_{TRN}$ converged toward similar values (Fig. 4). This suggests phytoplankton reliance on recycled N derived from the DON pool, which would push $\delta^{15}N_{POM}$ to lower values. A similar convergence of $\delta^{15}N_{POM}$ and $\delta^{15}N_{TRN}$ occurred at Sta. WE9 from 8/10 to 9/7, when [NO_3^-] was also nearly zero, again suggesting phytoplankton usage of DON. This reliance on regenerated N is supported by previous work in Lake Erie (Hoffman et al. 2022) and in other eutrophic lake systems such as Lake Taihu (Hampel et al. 2018) and Lake Champlain (McCarthy et al. 2013).

Sources of nitrate in Western Lake Erie

Riverine discharge is the major influence underpinning the patterns observed in $\delta^{15}N$ values of nitrate, and to a lesser extent, in DON and POM (Fig. 5). $\delta^{15}N$ values of nitrate form a spatial gradient between near and offshore stations that is strongly, positively correlated with conductivity (Fig. 5A). This suggests two isotopically distinct NO_3^- sources: an isotopically heavier source originating from the Maumee River, and a lighter source associated with the Detroit River. The higher $\delta^{15}N$ values from the Maumee likely result from agricultural land use, including increased application of manure and organic N-based fertilizers (Millar et al. 2014). Measurements of Detroit River water $\delta^{15}N_{NO3}$ averaged 2.4‰ in a recent study (Colborne et al. 2019), but the reasons for these low values are not fully known. Low $\delta^{15}N_{NO3}$ values were previously observed in Lake Superior, with mean values of −4.1‰ (Ostrom et al. 1998) and −2.3‰ (Finlay et al. 2007), interpreted as resulting from in-lake nitrification of ammonium/reduced N in rain and runoff (Finlay et al. 2007). The Detroit River connects the upstream lakes of Superior, Michigan, and Huron to downstream Lake Erie (via Lake St. Clair), so Detroit River $\delta^{15}N_{NO3}$ values could be partially due to propagation of $\delta^{15}N_{NO3}$ signature from Lake Superior.

Although $\delta^{18}O_{NO3}$ is often used to differentiate between sources that overlap in $\delta^{15}N_{NO3}$, both biological uptake and N cycling processes like nitrification, which is dominant in oxygenated environments, can blur initial isotopic compositions of both $\delta^{15}N$ and $\delta^{18}O$. The range of $\delta^{18}O_{NO3}$ values in our data are consistent with NO_3^- originating from nitrification, either in soils or rivers/lakes, but the lack of separation in $\delta^{18}O_{NO3}$ values between samples or stations makes it difficult to quantify relative contributions of potential NO_3^- sources. The data show little evidence for *direct* contributions from either atmospheric NO_3^- or nitrate-based fertilizers to Western Lake Erie (Supporting Information Fig. S5). This could reflect decreasing usage of nitrate-based fertilizers in agriculture (Cao et al. 2018). However, depending on the timing and nature of fertilizer application, NO_3^- from fertilizers may also be mixed into the soil N pool before being transported to rivers and lakes, with plant or soil microbial N cycling processes obscuring the original isotope signature before reaching the lake (Deutsch et al. 2006). Isotope measurements of potential NO_3^- source endmembers (e.g., soils, storm drains, river water) in the Maumee and Detroit River watersheds may allow better deconvolution of Western Lake Erie NO_3^- sources.

NO_3^- concentrations were not correlated with microcystin concentrations, but there was a positive correlation between microcystin concentrations and $\delta^{15}N_{POM}$ (Fig. 7B), suggesting that the N sources linked to microcystin production had higher $\delta^{15}N$ values. Most toxin production occurred at the nearshore Stas. WE9 and WE2 (Supporting Information Fig. S1), where phytoplankton were likely relying on isotopically heavier N substrates originating from the Maumee River. This is supported by a positive correlation between $\delta^{15}N_{NO3}$ and microcystin concentrations (Fig. 7A). Isotopically heavy ammonium could also be a N substrate for toxigenic *Microcystis*, as was observed in other systems (Lehman et al. 2015). Future work should examine whether this relationship holds in years with stronger and more extensive blooms.

DON sources and composition in Western Lake Erie

The temporal variability in DON concentrations and N isotope composition suggests a dynamic DON pool, and that some components are bioavailable on a seasonal timescale. This contrasts with trends observed in less eutrophic systems, where $\delta^{15}N_{TRN}$ and [DON] remained nearly constant; these include a subarctic lake (Gu 2012) and in the subtropical oceans (Knapp et al. 2005). Concentrations of DON in Western Lake Erie (8.5–57.5 μM) were within the lower end of the large range previously reported for freshwater lakes (4.0–200 μM Feuerstein et al. 1997; Berman and Bronk 2003; Zhang et al. 2015); concentrations as high as 327 μM were reported in hypereutrophic Lake Taihu (Yao et al. 2020). There are limited $\delta^{15}N$ measurements of DON in lakes, but the Western Lake Erie $\delta^{15}N_{TRN}$ values are similar to data from Lake Michigan, USA (2.6–5.8‰; Feuerstein et al. 1997) and Lake Suwa, Japan (7.3‰; Yoshioka et al. 1988), both of which are influenced by human activity and land use. DON $\delta^{15}N$ values lower than those in Western Lake Erie were observed in Lake Superior (−1.2‰, Feuerstein et al. 1997) and in Lake Kizaki, Japan (3.0‰; Yoshioka et al. 1988), which are less anthropogenically influenced.

Work in the marine environment has shown that processes such as cell lysis or particle solubilization that produce fresh

19395590, 2023, 4, Downloaded from https://aslopubs.onlinelibrary.wiley.com/doi/10.1002/lno.12311 by Wheaton College Ma, Wiley Online Library on [07/11/2024]. See the Terms and Conditions (https://onlinelibrary.wiley.com/terms-and-conditions) on Wiley Online Library for rules of use; OA articles are governed by the applicable Creative Commons License

DON from POM are nonfractionating and result in DON with a similar $\delta^{15}N$ value to the POM from which it is derived (Fawcett et al. 2011; Knapp et al. 2011). In contrast, there is likely isotope fractionation associated with processes that break down existing DON molecules to produce biologically available forms of N, for example, via deamination or hydrolysis of peptide bonds (Macko et al. 1986; Bada et al. 1989). Such reaction pathways are highly expressed in the *Microcystis*-associated microbiome (Smith et al. 2022), and would result in the release of isotopically lighter DON components like small peptides or ammonium that could be more accessible to phytoplankton, especially *Microcystis*. High NH_4^+ regeneration rates recently measured in Lake Erie (Hoffman et al. 2022) support active breakdown of DON via these types of reactions, and incorporation of this isotopically lighter material by phytoplankton would produce the relatively lower $\delta^{15}N_{POM}$ values we observed.

Considering the above, the pattern of $\delta^{15}N_{TRN} \leq \delta^{15}N_{POM}$ suggests that much of DON derives from POM. DON cycling in Western Lake Erie is probably complex, with many reactions that could influence $\delta^{15}N_{TRN}$, and it is difficult to identify specific processes from bulk isotope values. However, the positive direction of the relationship between [TRN] and $\delta^{15}N_{TRN}$ (Supporting Information Fig. S6) argues against a fractionating removal process, such as phytoplankton uptake, as the major control on $\delta^{15}N_{TRN}$. Such a process would instead produce a negative correlation by removing ^{14}N and leaving residual DON enriched in ^{15}N. Therefore, instead of a spring pulse of DON followed by processing and removal throughout the summer, the isotope data suggest continual in situ production of DON from POM at each station, with $\delta^{15}N_{TRN}$ values reflecting the trend of higher to lower $\delta^{15}N_{POM}$ and $\delta^{15}N_{NO3}$ values from nearshore to offshore stations (Fig. 5). This is supported by the nearshore to offshore increase in the Peak T/A ratio, which indicates there is more of the amino acid-like fraction of DOM relative to soil-derived OM (Supporting Information Fig. S4). Previous work in Lake Erie identified a similar pattern, which is explained by more sinks and fewer sources for Peak A material than for Peak T material in the lake (Cory et al. 2016, and references therein). However, given the strong positive relationship between specific conductivity and Peak T (Supporting Information Fig. S3), a fraction of the DON pool must be terrestrial or riverine in origin and could also be isotopically lighter than POM. The size of this terrestrial fraction is difficult to estimate from the data here, because the FDOM proxies are not quantitative. [DON] is moderately correlated with both specific conductivity ($r_s = 0.61$ $p = 2 \times 10^{-5}$), and with Peak T ($r_s = 0.62$, $p = 1.75 \times 10^{-5}$). One possible explanation of these observations is that Peak T represents a mostly terrestrial fraction of DON that is more conservative than the bulk DON pool, leading to a strong relationship between Peak T DON and conductivity. However, in situ production of DON from POM could produce both additional Peak T DON and nonfluorescent DON, resulting in weaker correlations between [DON] and both Peak T and specific conductivity. Future measurements of riverine FDOM, and riverine DON isotopic and molecular composition, could help constrain how much of the DON pool originates from terrestrial vs. in-lake sources.

Conclusions

This study tracked sources and forms of N during progression of the cyanoHAB in Lake Erie. The results suggest that NO_3^- was a greater contributor to phytoplankton biomass than DON, and that riverine input was the primary influence on NO_3^- $\delta^{15}N$ values in Western Lake Erie, with little effect from biological processes. Toxin concentrations were positively correlated with $\delta^{15}N$ values of POM and NO_3^-, suggesting that toxin-producing cyanobacteria relied on isotopically heavier N substrates sourced from the Maumee River. The DON pool in Lake Erie was spatially and temporally dynamic, and the fraction of DON in the total dissolved N pool increased from early to late summer. Much of the DON was likely autochthonous material derived from POM, and became a more important N substrate for phytoplankton in late summer after depletion of NO_3^-.

These results support previous work on the importance of regenerated N in the longevity of cyanoHABs (Hampel et al. 2018, 2019; Hoffman et al. 2022). Although the interpretive power of bulk measurements is limited, the patterns identified here provide a starting point for future work examining how both external and internal N sources fuel blooms in Western Lake Erie. For example, combining metatranscriptomics with chemical and isotopic measurements of N substrates and POM would enable us to address how the shift from NO_3^- to DON may be connected to previously observed community shifts in cyanobacterial strain diversity (Yancey et al. 2022). In addition, DON is a complex mixture of molecules spanning a wide range of labilities, and mechanisms *Microcystis* use to access DON during the bloom remain mostly unknown, including the potential role of *Microcystis*-associated heterotrophic bacteria in releasing bioavailable N compounds from DON (Purvina et al. 2010; Hoke et al. 2021; Smith et al. 2022). Finally, concentration, isotope, and even 'omics measurements are "snapshots" that may not capture quickly cycling material such as labile components of DON and regenerated ammonium. Future studies should balance these techniques with measurements of N uptake and regeneration rates, which are likely especially critical for understanding late-stage bloom dynamics.

Data availability statement

All data generated and analyzed during the current study are available in the University of Michigan's Deep Blue repository (https://doi.org/10.7302/mg4b-x721) and are also reported in Supporting Information Tables S1 and S2.

19395590, 2023, 4, Downloaded from https://aslopubs.onlinelibrary.wiley.com/doi/10.1002/lno.12311 by Wheaton College Ma, Wiley Online Library on [07/11/2024]. See the Terms and Conditions (https://onlinelibrary.wiley.com/terms-and-conditions) on Wiley Online Library for rules of use; OA articles are governed by the applicable Creative Commons License

References

Allinger, L. E., and E. D. Reavie. 2013. The ecological history of Lake Erie as recorded by the phytoplankton community. J. Great Lakes Res. **39**: 365–382. doi:10.1016/j.jglr.2013.06.014

Bada, J. L., M. J. Schoeninger, and A. Schimmelmann. 1989. Isotopic fractionation during peptide bond hydrolysis. Geochim. Cosmochim. Acta **53**: 3337–3341. doi:10.1016/0016-7037(89)90114-2

Belisle, B. S., M. M. Steffen, H. L. Pound, S. B. Watson, J. M. DeBruyn, R. A. Bourbonniere, G. L. Boyer, and S. W. Wilhelm. 2016. Urea in Lake Erie: Organic nutrient sources as potentially important drivers of phytoplankton biomass. J. Great Lakes Res. **42**: 599–607. doi:10.1016/j.jglr.2016.03.002

Berman, T., and D. A. Bronk. 2003. Dissolved organic nitrogen: A dynamic participant in aquatic ecosystems. Aquat. Microb. Ecol. **31**: 279–305. doi:10.3354/ame031279

Berry, M. A., and others. 2017. Cyanobacterial harmful algal blooms are a biological disturbance to Western Lake Erie bacterial communities. Environ. Microbiol. **19**: 1149–1162. doi:10.1111/1462-2920.13640

Beutler, M., K. Wiltshire, B. Meyer, C. Moldaenke, C. Lüring, M. Meyerhöfer, U. P. Hansen, and H. Dau. 2002. A fluorometric method for the differentiation of algal populations in vivo and in situ. Photosynth. Res. **72**: 39–53. doi:10.1023/a:1016026607048

Beversdorf, L. J., T. R. Miller, and K. D. McMahon. 2015. Long-term monitoring reveals carbon-nitrogen metabolism key to microcystin production in eutrophic lakes. Front. Microbiol. **6**. doi:10.3389/fmicb.2015.00456

Blomqvist, P., A. Pettersson, and P. Hyenstrane. 1994. Ammonium-nitrogen: A key regulatory factor causing dominance of non-nitrogen-fixing cyanobacteria in aquatic systems. Arch. Hydrobiol. **132**: 141–164.

Burtner, A., C. Kitchens, G. Carter, K. McCabe, H. Henderson, C. Godwin, D. Gossiaux, and R. Errera. 2022. Physical, chemical, and biological water quality monitoring data to support detection of harmful algal blooms (HABs) physical, chemical, and biological water quality data collected from a small boat in western Lake Erie, Great Lakes from 2020-06-16 to 2021-10-27 (NCEI Accession 0254720). NOAA National Centers for Environmental Information. Dataset. https://www.ncei.noaa.gov/archive/accession/0254720

Cao, P., C. Lu, and Z. Yu. 2018. Historical nitrogen fertilizer use in agricultural ecosystems of the contiguous United States during 1850–2015: Application rate, timing, and fertilizer types. Earth Syst. Sci. Data **10**: 969–984. doi:10.5194/ESSD-10-969-2018

Casciotti, K. L., D. M. Sigman, M. G. Hastings, J. K. Böhlke, and A. Hilkert. 2002. Measurement of the oxygen isotopic composition of nitrate in seawater and freshwater using the denitrifier method. Anal. Chem. **74**: 4905–4912. doi:10.1021/ac020113w

Chaffin, J. D., T. B. Bridgeman, and D. L. Bade. 2013. Nitrogen constrains the growth of late summer cyanobacterial blooms in Lake Erie. Adv. Microbiol. **2013**: 16–26. doi:10.4236/AIM.2013.36A003

Chaffin, J. D., and T. B. Bridgeman. 2014. Organic and inorganic nitrogen utilization by nitrogen-stressed cyanobacteria during bloom conditions. J. Appl. Phycol. **26**: 299–309. doi:10.1007/s10811-013-0118-0

Chernoff, N., D. Hill, J. Lang, J. Schmid, T. Le, A. Farthing, and H. Huang. 2020. The comparative toxicity of 10 microcystin congeners administered orally to mice: Clinical effects and organ toxicity. Toxins **12**: 403. doi:10.3390/TOXINS12060403

Colborne, S. F., and others. 2019. Water and sediment as sources of phosphate in aquatic ecosystems: The Detroit River and its role in the Laurentian Great Lakes. Sci. Total Environ. **647**: 1594–1603. doi:10.1016/j.scitotenv.2018.08.029

Cory, R. M., and others. 2016. Seasonal dynamics in dissolved organic matter, hydrogen peroxide, and cyanobacterial blooms in Lake Erie. Front. Mar. Sci. **3**: 1–17. doi:10.3389/fmars.2016.00054

Davis, T. W., D. L. Berry, G. L. Boyer, and C. J. Gobler. 2009. The effects of temperature and nutrients on the growth and dynamics of toxic and non-toxic strains of *Microcystis* during cyanobacteria blooms. Harmful Algae **8**: 715–725. doi:10.1016/j.hal.2009.02.004

Davis, T. W., G. S. Bullerjahn, T. Tuttle, R. M. McKay, and S. B. Watson. 2015. Effects of increasing nitrogen and phosphorus concentrations on phytoplankton community growth and toxicity during Planktothrix blooms in Sandusky Bay, Lake Erie. Environ. Sci. Technol. **49**: 7197–7207. doi:10.1021/acs.est.5b00799

Deutsch, B., M. Mewes, I. Liskow, and M. Voss. 2006. Quantification of diffuse nitrate inputs into a small river system using stable isotopes of oxygen and nitrogen in nitrate. Org. Geochem. **37**: 1333–1342. doi:10.1016/J.ORGGEOCHEM.2006.04.012

Donald, D. B., M. J. Bogard, K. Finlay, and P. R. Leavitt. 2011. Comparative effects of urea, ammonium, and nitrate on phytoplankton abundance, community composition, and toxicity in hypereutrophic freshwaters. Limnol. Oceanogr. **56**: 2161–2175. doi:10.4319/LO.2011.56.6.2161

Downing, T. G., C. Meyer, M. M. Gehringer, and M. Van De Venter. 2005. Microcystin content of *Microcystis aeruginosa* is modulated by nitrogen uptake rate relative to specific growth rate or carbon fixation rate. Environ. Toxicol. **20**: 257–262.

Durand, P., and others. 2011. Nitrogen processes in aquatic ecosystems, p. 126–146. *In* M. Sutton and others [eds.], The European Nitrogen Assessment: Sources, effects and policy

19395590, 2023, 4, Downloaded from https://aslopubs.onlinelibrary.wiley.com/doi/10.1002/lno.12311 by Wheaton College Ma, Wiley Online Library on [07/11/2024]. See the Terms and Conditions (https://onlinelibrary.wiley.com/terms-and-conditions) on Wiley Online Library for rules of use; OA articles are governed by the applicable Creative Commons License

perspectives. Cambridge University Press. doi:10.1017/cbo9780511976988.010

Escoffier, N., C. Bernard, S. Hamlaoui, A. Groleau, and A. Catherine. 2015. Quantifying phytoplankton communities using spectral fluorescence: The effects of species composition and physiological state. J. Plankton Res. **37**: 233–247. doi:10.1093/plankt/fbu085

Fawcett, S. E., M. W. Lomas, J. R. Casey, B. B. Ward, and D. M. Sigman. 2011. Assimilation of upwelled nitrate by small eukaryotes in the Sargasso Sea. Nat. Geosci. **4**: 717–722. doi:10.1038/ngeo1265

Fellman, J. B., E. Hood, D. V. D'Amore, R. T. Edwards, and D. White. 2009. Seasonal changes in the chemical quality and biodegradability of dissolved organic matter exported from soils to streams in coastal temperate rainforest watersheds. Biogeochemistry **95**: 277–293. doi:10.1007/s10533-009-9336-6

Feuerstein, T. P., P. H. Ostrom, and N. E. Ostrom. 1997. Isotopic biogeochemistry of dissolved organic nitrogen: A new technique and application. Org. Geochem. **27**: 363–370. doi:10.1016/S0146-6380(97)00071-5

Finlay, J. C., and C. Kendall. 2007. Stable isotope tracing of temporal and spatial variability in organic matter sources to freshwater ecosystems, p. 283–333. *In* Stable isotopes in ecology and environmental science, 2nd ed. Wiley-Blackwell.

Finlay, J. C., R. W. Sterner, and S. Kumar. 2007. Isotopic evidence for in-lake production of accumulating nitrate in lake superior. Ecol. Appl. **17**: 2323–2332. doi:10.1890/07-0245.1

Flores, E., and A. Herrero. 2005. Nitrogen assimilation and nitrogen control in cyanobacteria. Biochem. Soc. Trans. **33**: 164–167. doi:10.1042/BST0330164

Fogel, M. L., and L. A. Cifuentes. 1993. Isotope fractionation during primary production, p. 73–98. Organic geochemistry: Principles and applications, Springer.

Glibert, P. M., and others. 2016. Pluses and minuses of ammonium and nitrate uptake and assimilation by phytoplankton and implications for productivity and community composition, with emphasis on nitrogen-enriched conditions. Limnol. Oceanogr. **61**: 165–197. doi:10.1002/lno.10203

GLWQA (Great Lakes Water Quality Agreement). 2016. The United States and Canada adopt phosphorus load reduction targets to combat lake erie algal blooms. Recommended binational phosphorous targets to combat Lake Erie algal blooms. Factsheet. Available at https://binational.net/wp-content/uploads/2015/07/nutrients-factsheet-en-FINAL.pdf.

Gobler, C. J., J. A. M. Burkholder, T. W. Davis, M. J. Harke, T. Johengen, C. A. Stow, and D. B. Van de Waal. 2016. The dual role of nitrogen supply in controlling the growth and toxicity of cyanobacterial blooms. Harmful Algae **54**: 87–97. doi:10.1016/j.hal.2016.01.010

Granger, J., D. M. Sigman, M. M. Rohde, M. T. Maldonado, and P. D. Tortell. 2010. N and O isotope effects during nitrate assimilation by unicellular prokaryotic and eukaryotic plankton cultures. Geochim. Cosmochim. Acta **74**: 1030–1040. doi:10.1016/j.gca.2009.10.044

Gu, B. 2012. Stable isotopes as indicators for seasonally dominant nitrogen cycling processes in a subarctic lake. Int. Rev. Hydrobiol. **97**: 233–243. doi:10.1002/iroh.201111466

Hampel, J. J., M. J. McCarthy, W. S. Gardner, L. Zhang, H. Xu, G. Zhu, and S. E. Newell. 2018. Nitrification and ammonium dynamics in Taihu Lake, China: Seasonal competition for ammonium between nitrifiers and cyanobacteria. Biogeosciences **15**: 733–748. doi:10.5194/bg-15-733-2018

Hampel, J. J., M. J. McCarthy, M. Neudeck, G. S. Bullerjahn, R. M. L. McKay, and S. E. Newell. 2019. Ammonium recycling supports toxic Planktothrix blooms in Sandusky Bay, Lake Erie: Evidence from stable isotope and metatranscriptome data. Harmful Algae **81**: 42–52. doi:10.1016/j.hal.2018.11.011

Harke, M. J., and C. J. Gobler. 2015. Daily transcriptome changes reveal the role of nitrogen in controlling microcystin synthesis and nutrient transport in the toxic cyanobacterium, *Microcystis aeruginosa*. BMC Genomics **16**: 1–18. doi:10.1186/s12864-015-2275-9

Hoffman, D. K., M. J. McCarthy, A. R. Boedecker, J. A. Myers, and S. E. Newell. 2022. The role of internal nitrogen loading in supporting non-N-fixing harmful cyanobacterial blooms in the water column of a large eutrophic lake. Limnol. Oceanogr. **67**: 2028–2041. doi:10.1002/LNO.12185

Hoke, A. K., and others. 2021. Genomic signatures of Lake Erie bacteria suggest interaction in the *Microcystis* phycosphere. PLoS One **16**: e0257017. doi:10.1371/JOURNAL.PONE.0257017

Horst, G. P., O. Sarnelle, J. D. White, S. K. Hamilton, R. R. B. Kaul, and J. D. Bressie. 2014. Nitrogen availability increases the toxin quota of a harmful cyanobacterium, *Microcystis aeruginosa*. Water Res. **54**: 188–198. doi:10.1016/j.watres.2014.01.063

Hou, X., L. Feng, Y. Dai, and others. 2022. Global mapping reveals increase in lacustrine algal blooms over the past decade. Nat. Geosci. **15**: 130–134. doi:10.1038/s41561-021-00887-x

Jankowiak, J., T. Hattenrath-Lehmann, B. J. Kramer, M. Ladds, and C. J. Gobler. 2019. Deciphering the effects of nitrogen, phosphorus, and temperature on cyanobacterial bloom intensification, diversity, and toxicity in western Lake Erie. Limnol. Oceanogr. **64**: 1347–1370. doi:10.1002/LNO.11120

Kane, D. D., J. D. Conroy, R. P. Richards, D. B. Baker, and D. A. Culver. 2014. Re-eutrophication of Lake Erie: Correlations between tributary nutrient loads and phytoplankton biomass. J. Great Lakes Res. **40**: 496–501.

19395590, 2023, 4, Downloaded from https://aslopubs.onlinelibrary.wiley.com/doi/10.1002/lno.12311 by Wheaton College Ma, Wiley Online Library on [07/11/2024]. See the Terms and Conditions (https://onlinelibrary.wiley.com/terms-and-conditions) on Wiley Online Library for rules of use; OA articles are governed by the applicable Creative Commons License

Kassambara, A. 2020. ggpubr: "ggplot2" based publication ready plots. R package version 0.4.0. Available from https://cran.r-project.org/package=ggpubr

Kendall, C., E. M. Elliott, and S. D. Wankel. 2007. Tracing anthropogenic inputs of nitrogen to ecosystems, p. 375–449. *In* Stable isotopes in ecology and environmental science, 2nd ed. Wiley-Blackwell.

Knapp, A. N., D. M. Sigman, and F. Lipschultz. 2005. N isotopic composition of dissolved organic nitrogen and nitrate at the Bermuda Atlantic time-series study site. Global Biogeochem. Cycl. **19**: 1–15. doi:10.1029/2004GB002320

Knapp, A. N., D. M. Sigman, F. Lipschultz, A. B. Kustka, and D. G. Capone. 2011. Interbasin isotopic correspondence between upper-ocean bulk DON and subsurface nitrate and its implications for marine nitrogen cycling. Global Biogeochem. Cycl. **25**: GB4004. doi:10.1029/2010GB003878

Lehmann, M. F., S. M. Bernasconi, J. A. McKenzie, A. Barbieri, M. Simona, and M. Veronesi. 2004. Seasonal variation of the $\delta^{13}C$ and $\delta^{15}N$ of particulate and dissolved carbon and nitrogen in Lake Lugano: Constraints on biogeochemical cycling in a eutrophic lake. Limnol. Oceanogr. **49**: 415–429. doi:10.4319/lo.2004.49.2.0415

Lehman, P. W., C. Kendall, M. A. Guerin, M. B. Young, S. R. Silva, G. L. Boyer, and S. J. Teh. 2015. Characterization of the *Microcystis* bloom and its nitrogen supply in San Francisco Estuary using stable isotopes. Estuar. Coast. **38**: 165–178. doi:10.1007/s12237-014-9811-8

Maccoux, M. J., A. Dove, S. M. Backus, and D. M. Dolan. 2016. Total and soluble reactive phosphorus loadings to Lake Erie: A detailed accounting by year, basin, country, and tributary. J. Great Lakes Res. **42**: 1151–1165. doi:10.1016/J.JGLR.2016.08.005

Macko, S. A., M. L. F. Estep, M. H. Engel, and P. E. Hare. 1986. Kinetic fractionation of stable nitrogen isotopes during amino acid transamination. Geochim. Cosmochim. Acta **50**: 2143–2146. doi:10.1016/0016-7037(86)90068-2

McCarthy, M. J., W. S. Gardner, M. F. Lehmann, and D. F. Bird. 2013. Implications of water column ammonium uptake and regeneration for the nitrogen budget in temperate, eutrophic Missisquoi Bay, Lake Champlain (Canada/USA). Hydrobiologia **718**: 173–188. doi:10.1007/s10750-013-1614-6

McCusker, E. M., P. H. Ostrom, N. E. Ostrom, J. D. Jeremiason, and J. E. Baker. 1999. Seasonal variation in the biogeochemical cycling of seston in Grand Traverse Bay, Lake Michigan. Org. Geochem. **30**: 1543–1557. doi:10.1016/S0146-6380(99)00129-1

Millar, N., J. E. Doll, and G. P. Robertson. 2014. Management of nitrogen fertilizer to reduce nitrous oxide emissions from field crops. Climate Change and Agriculture Fact Sheet Series—MSU Extension Bulletin E3152.

Monchamp, M.-E., F. R. Pick, B. E. Beisner, and R. Maranger. 2014. Nitrogen forms influence microcystin concentration and composition via changes in cyanobacterial community structure. PLoS One **9**: e85573. doi:10.1371/journal.pone.0085573

Newell, S. E., T. W. Davis, T. H. Johengen, D. Gossiaux, A. Burtner, D. Palladino, and M. J. McCarthy. 2019. Reduced forms of nitrogen are a driver of non-nitrogen-fixing harmful cyanobacterial blooms and toxicity in Lake Erie. Harmful Algae **81**: 86–93. doi:10.1016/j.hal.2018.11.003

NOAA-NCCOS. 2020. Lake Erie Algal Bloom was Mild, as Predicted by Seasonal Forecast. https://coastalscience.noaa.gov/news/lake-erie-hab-2020-bloom-severity-was-mild-as-predicted-by-seasonal-forecast/ [Accessed 20 March 2021].

Ostrom, N. E., S. A. Macko, D. Deibel, and R. J. Thompson. 1997. Seasonal variation in the stable carbon and nitrogen isotope biogeochemistry of a coastal cold ocean environment. Geochim. Cosmochim. Acta **61**: 2929–2942. doi:10.1016/S0016-7037(97)00131-2

Ostrom, N. E., D. T. Long, E. M. Bell, and T. Beals. 1998. The origin and cycling of particulate and sedimentary organic matter and nitrate in Lake Superior. Chem. Geol. **152**: 13–28. doi:10.1016/S0009-2541(98)00093-X

Purvina, S., C. Béchemin, M. Balode, C. Verite, C. Arnaud, and S. Y. Maestrini. 2010. Release of available nitrogen from river-discharged dissolved organic matter by heterotrophic bacteria associated with the cyanobacterium *Microcystis aeruginosa*. Estonian J. Ecol. **59**: 184–196. doi:10.3176/eco.2010.3.02

R Core Team. 2022. R: A language and environment for statistical computing. R Foundation for Statistical Computing,. Available from https://www.r-project.org/.

Scavia, D., and others. 2016. Informing Lake Erie agriculture nutrient management via scenario evaluation. http://graham.umich.edu/media/pubs/InformingLakeErieAgricultureNutrientManagementviaScenarioEvaluation.pdf

Sigman, D., K. Karsh, and K. Casciotti. 2009. Ocean process tracers: Nitrogen isotopes in the ocean, Elsevier, p. 4138–4153. *In* Encyclopedia of ocean sciences.

Smith, D. J., J. J. Kharbush, R. D. Kersten, G., and J. Dick. 2022. Uptake of phytoplankton-derived carbon and cobalamins by novel *Acidobacteria* genera in *Microcystis* blooms inferred from metagenomic and metatranscriptomic evidence. Appl. Environ. Microbiol. **88**: 1–18. doi:10.1128/aem.01803-21

Sterner, R. W. 2021. The laurentian great lakes: A biogeochemical test bed. Annu. Rev. Earth Planet. Sci. **49**: 201–229. doi:10.1146/annurev-earth-071420-051746

Stow, C. A., Y. Cha, L. T. Johnson, R. Confesor, and R. P. Richards. 2015. Long-term and seasonal trend decomposition of Maumee river nutrient inputs to western Lake Erie. Environ. Sci. Technol. **49**: 3392–3400. doi:10.1021/es5062648

Stumpf, R. P., L. T. Johnson, T. T. Wynne, and D. B. Baker. 2016. Forecasting annual cyanobacterial bloom biomass to inform management decisions in Lake Erie. J. Great Lakes Res. **42**: 1174–1183. doi:10.1016/J.JGLR.2016.08.006

19395590, 2023, 4, Downloaded from https://aslopubs.onlinelibrary.wiley.com/doi/10.1002/lno.12311 by Wheaton College Ma, Wiley Online Library on [07/11/2024]. See the Terms and Conditions (https://onlinelibrary.wiley.com/terms-and-conditions) on Wiley Online Library for rules of use; OA articles are governed by the applicable Creative Commons License

Teranes, J. L., and S. M. Bernasconi. 2000. The record of nitrate utilization and productivity limitation provided by d15N values in lake organic matter—A study of sediment trap and core sediments from Baldeggersee, Switzerland. Limnol. Oceanogr. **45**: 801–813. doi:10.4319/lo.2000.45.4.0801

Wickham, H., R. Francois, L. Henry, and K. Müller. 2022. dplyr: A grammer of data manipulation. R package version 1.0.10. Available from https://cran.r-project.org/package=dplyr.

Yamashita, Y., and E. Tanoue. 2003. Chemical characterization of protein-like fluorophores in DOM in relation to aromatic amino acids. Mar. Chem. **82**: 255–271. doi:10.1016/S0304-4203(03)00073-2

Yancey, C. E., and others. 2022. Metagenomic and metatranscriptomic insights into population diversity of *Microcystis* blooms: Spatial and temporal dynamics of mcy genotypes, including a partial operon that can be abundant and expressed. Appl. Environ. Microbiol. **88**: e0246421. doi:10.1128/AEM.02464-21

Yao, X., Y. Zhang, L. Zhang, G. Zhu, B. Qin, Y. Zhou, and J. Xue. 2020. Emerging role of dissolved organic nitrogen in supporting algal bloom persistence in Lake Taihu, China: Emphasis on internal transformations. Sci. Total Environ. **736**: 139497. doi:10.1016/j.scitotenv.2020.139497

Yoshioka, T., E. Wada, and Y. Saijo. 1988. Isotopic characterization of Lake Kizaki and Lake Suwa. Jpn. J. Limnol. (Rikusuigaku Zasshi) **49**: 119–128. doi:10.3739/rikusui.49.119

Zhang, Y., S. Huo, F. Zan, B. Xi, and J. Zhang. 2015. Dissolved organic nitrogen (DON) in seventeen shallow lakes of Eastern China. Environ. Earth Sci. **74**: 4011–4021. doi:10.1007/s12665-015-4185-1

Acknowledgments

The authors thank NOAA-GLERL staff for collection of water samples, and Roger Patrick Kelley, Catherine Polik, and Dhurba Pandey for their help with sample processing. The authors thank Prof. Rose Cory for providing CDOM/FDOM measurements, which were supported by NSF-BioOce grant 1736629. IRMS analyses and S.J.C. were supported by Harvard University.

Conflict of Interest

We have no conflicts of interest to report.

Submitted 15 July 2022
Revised 17 October 2022
Accepted 12 January 2023

Associate editor: Kimberly Van Meter

19395590, 2023, 4, Downloaded from https://aslopubs.onlinelibrary.wiley.com/doi/10.1002/lno.12311 by Wheaton College Ma, Wiley Online Library on [07/11/2024]. See the Terms and Conditions (https://onlinelibrary.wiley.com/terms-and-conditions) on Wiley Online Library for rules of use; OA articles are governed by the applicable Creative Commons License